J|A|C|S ARTICLES

Published on Web 06/28/2010

Nonhumidified Intermediate Temperature Fuel Cells Using Protic Ionic Liquids

Seung-Yul Lee, Atsushi Ogawa, Michihiro Kanno, Hirofumi Nakamoto, Tomohiro Yasuda, and Masayoshi Watanabe*

Department of Chemistry and Biotechnology, Yokohama National University, 79-5 Tokiwadai, Hodogaya-ku, Yokohama 240-8501, Japan

Received March 21, 2010; E-mail: mwatanab@ynu.ac.jp

Abstract: In this paper, the characterization of a protic ionic liquid, diethylmethylammonium trifluoromethanesulfonate ([dema][TfO]), as a proton conductor for a fuel cell and the fabrication of a membrane-type fuel cell system using [dema][TfO] under nonhumidified conditions at intermediate temperatures are described in detail. In terms of physicochemical and electrochemical properties, [dema][TfO] exhibits high activity for fuel cell electrode reactions (i.e., the hydrogen oxidation reaction (HOR) and oxygen reduction reaction (ORR)) at a Pt electrode, and the open circuit voltage (OCV) of a liquid fuel cell is 1.03 V at 150 °C, as has reported in ref 27. However, diethylmethylammonium bis(trifluoromethane sulfonyl)amide ([dema][NTf_2]) has relatively low HOR and ORR activity, and thus, the OCV is ca. 0.7 V, although [dema][NTf_2] and [dema][TfO] have an identical cation ([dema]) and similar thermal and bulk-transport properties. Proton conduction occurs mainly via the vehicle mechanism in [dema][TfO] and the proton transference number (t_+) is 0.5−0.6. This relatively low t_+ appears to be more disadvantageous for a proton conductor than for other electrolytes such as hydrated sulfonated polymer electrolyte membranes ($t_+ = 1.0$). However, fast proton-exchange reactions occur between ammonium cations and amines in a model compound. This indicates that the proton-exchange mechanism contributes to the fuel cell system under operation, where deprotonated amines are continuously generated by the cathodic reaction, and that polarization of the cell is avoided. Six-membered sulfonated polyimides in the diethylmethylammonium form exhibit excellent compatibility with [dema][TfO]. The composite membranes can be obtained up to a [dema][TfO] content of 80 wt % and exhibit good thermal stability, high ionic conductivity, and mechanical strength and gas permeation comparable to those of hydrated Nafion. H_2/O_2 fuel cells prepared using the composite membranes can successfully operate at temperatures from 30 to 140 °C under nonhumidified conditions, and a current density of 250 mA cm^{-2} is achieved at 120 °C. The protic ionic liquid and its composite membrane are a possible candidate for an electrolyte of a H_2/O_2 fuel cell that operates under nonhumidified conditions.

1. Introduction

A fuel cell system that can be operated at intermediate temperatures (>100 °C) without humidification is in great demand because it offers several advantages over current polymer electrolyte fuel cells.[1] First, water management becomes unnecessary, and thus the volume of the system can be reduced. Second, the activity of the Pt electrode catalyst can be improved at elevated temperatures, and poisoning from carbon monoxide can be reduced, leading to a reduction in the amount of Pt catalyst required. Third, the utilization of generated heat and temperature control of the cell by a radiator become easier. To realize such nonhumidified fuel cells, the development of a proton-conducting electrolyte is a key issue.

Phosphoric acid is one such proton conductor that possesses unique properties; phosphoric acid forms hydrogen bonding networks and partly self-dissociates (∼15%) to $H_4PO_4^+$ and $H_2PO_4^-$, which act as proton defects in the networks. This feature makes proton conduction via the Grotthuss mechanism possible even in the absence of water.[2] From the mid-1970s, great efforts have been devoted toward realizing phosphoric acid fuel cells (PAFCs),[3] and nowadays, PAFC electric power generation is employed in several factories around the world. Fabrication of phosphoric acid into membranes has been a critical issue and supports based on SiC have been widely used.[4] However, the resulting composite membranes simply absorbs phosphoric acid in the porous structure of SiC, and thus, phosphoric acid readily leaks out.

(1) (a) Li, Q.; He, R.; Jensen, J. O.; Bjerrum, N. J. *Chem. Mater.* **2003**, *15*, 4896. (b) Zhang, J.; Xie, Z.; Zhang, J.; Tang, Y.; Song, C.; Navessin, T.; Shi, Z.; Song, D.; Wang, H.; Wilkinson, D. P.; Liu, Z.-S.; Holdcroft, S. *J. Power Sources* **2006**, *160*, 872. (c) Hickner, M. A.; Ghassemi, H.; Kim, Y.-S.; Einsla, B. R.; McGrath, J. E. *Chem. Rev.* **2004**, *104*, 4587. (d) Yang, C.; Costamagna, P.; Srinivasam, S.; Benziger, J.; Bocarsly, A. B. *J. Power Sources* **2001**, *103*, 1.

(2) Gupta, S.; Tryk, D.; Bae, I.; Aldred, W.; Yeager, E. *J. Appl. Electrochem.* **1989**, *19*, 19.

(3) (a) Kreuer, K. D.; Paddison, S. J.; Spohr, E.; Schuster, M. *Chem. Rev.* **2004**, *104*, 4637. (b) Breault, R. D. *Handbook of Fuel Cells: Fundamentals Technology and Applications*; Vielstich, W., Lamm, A., Gasteiger, H. A., Eds.; J. Wiley & Sons: Chichester, 2003; Vol. 4, pp 797−810. (c) Larminie, J.; Dicks, A. *Fuel Cell Systems Explained*; J. Wiley & Sons: Chichester, 2000; pp 137−145.

10.1021/ja102367x

Scheme 1. Comparison of Aqueous Acidic Solutions and Protic Ionic Liquids

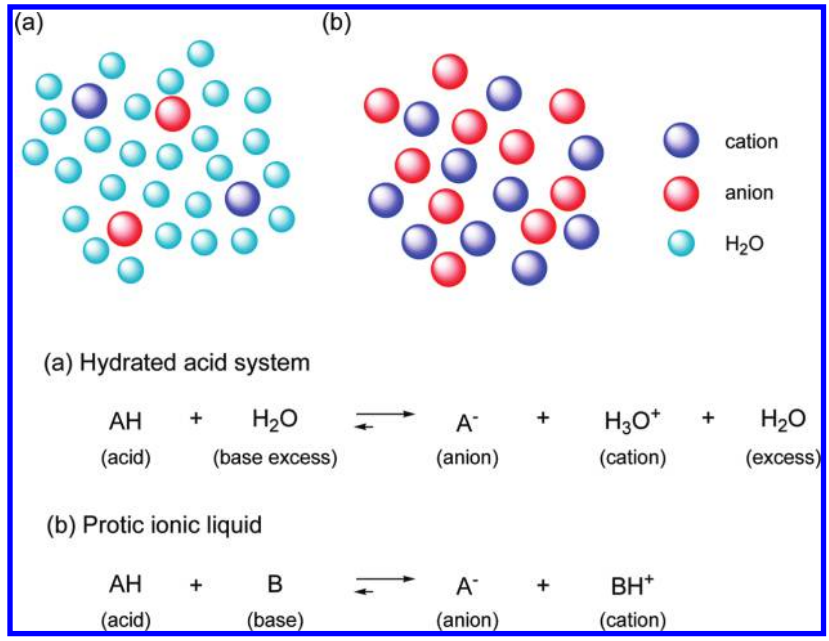

Phosphoric-acid-doped polybenzimidazole (PPA/PBI) was proposed in the 1990s.[5] In a PPA/PBI system, PBI acts as not only a matrix polymer but also a proton acceptor.[6] However, PPA/PBI exhibits high proton conductivity only when the polymer retains a large excess amount of phosphoric acid,[7] in which case free phosphoric acid exists and leakage is again a serious issue. Another concern with regard to PAFCs is their narrow range of operation temperatures. At temperatures higher than 150 °C, dehydration of phosphoric acid begins, resulting in the formation of poly(phosphoric acid), which exhibits poorer proton conductivity, and is in equilibrium with hydrolysis due to water existing in the system. At low temperatures, on the other hand, it is difficult to promote the electrode reactions because of the poisoning of the Pt catalyst with phosphoric acid.[8] Consequently, PAFCs are usually operated at ∼200 °C.

Solid acid proton conductors such as $CsHSO_4$ and CsH_2PO_4 have also been examined.[9] These conductors undergo solid−solid transition from normal crystal phase to plastic crystal phase below their melting temperatures (T_m) and exhibit high proton conduction via the Grotthuss mechanism in the plastic crystal phase. Haile and co-workers reported on the performance of fuel cells prepared using such inorganic proton conductors.[10] The solid−solid transition temperatures of $CsHSO_4$ and CsH_2PO_4 are 140 and 170 °C, respectively, and dehydration simultaneously occurs in the plastic crystal phases. Thus, humidification is necessary to increase the dehydration temperature and to continue fuel cell operation.

Hibino and co-workers studied MP_2O_7 (M: Sn, Ce, and Zr) as anhydrous proton conductors. They succeeded in fabricating thin membranes including $Sn_{0.95}Al_{0.05}P_2O_7$ by using sulfonated polystyrene-*b*-poly(ethylene/butylene)-*b*-polystyrene (sSEBS) and demonstrated that a fuel cell using the composite membrane can operate at temperatures from room temperature to 150 °C under nonhumidified conditions.[11]

Hagiwara and co-workers reported that ionic liquids, 1-ethyl-3-methylimidazorium fluorohydrogenate $(F(HF)_x^-$, $X = 1.3$ or 2.3), possess a proton transport property attributable to $F(HF)_x^-$ under anhydrous conditions.[12] They fabricated composite membranes using fluorinated matrix polymers and succeeded in achieving nonhumidified fuel cell operation at 120 °C with a current density of 100 mA cm^{-2}.[13]

Recently, one-dimensional imidazole aggregates in aluminum porous coordination polymers were found to exhibit high proton conductivity via the Grotthuss mechanism under anhydrous conditions.[14] Despite such studies, the development of novel proton-conducting materials with little or no dependence on humidity at temperatures above 100 °C still remains an important challenge to the realization of practical fuel cells.

Here, we reconsider the most common proton conductors (i.e., acidic aqueous systems), which include water-swollen polyelectrolyte membranes such as Nafion. In such an acidic aqueous system, water molecules act as a base for the acid and are protonated to form hydronium cations because the pK_a value

(4) (a) Song, R.-H.; Dheenadayalan, S.; Shin, D.-R. *J. Power Sources* **2002**, *106*, 167. (b) Caires, M. I.; Buzzo, M. L.; Ticianelli, E. A.; Gonzarez, E. R. *J. Appl. Electrochem.* **1997**, *27*, 19. (c) Yoon, K. H.; Yang, B. D. *J. Power Sources* **2003**, *124*, 47.
(5) (a) Wainright, J. S.; Wang, J.-T.; Weng, D.; Savinell, R. F.; Litt, M. *J. Electrochem. Soc.* **1995**, *142*, L121. (b) Wang, J.-T.; Savinell, R. F.; Wainright, J.; Litt, M.; Yu, H. *Electrochim. Acta* **1996**, *41*, 193. (c) Glipa, X.; Bonnet, B.; Mula, B.; Jones, D. J.; RozieÁre, J. *J. Mater. Chem.* **1999**, *9*, 3045. (d) Kawahara, M.; Rikukawa, M.; Sanui, K.; Ogata, N. *Solid State Ionics* **2000**, *136*−*137*, 1193.
(6) (a) Bouchet, R.; Siebert, E. *Solid State Ionics* **1999**, *118*, 287. (b) Kreuer, K. D.; Fuchs, A.; Ise, M.; Spaeth, M.; Maier, J. *Electrochim. Acta* **1998**, *43*, 1281.
(7) Ma, Y.-L.; Wainright, J. S.; Litt, M. H.; Savinell, R. F. *J. Electrochem. Soc.* **2004**, *151*, A8–A16.
(8) Zelenay, P.; Scharifker, B. R.; Bockris, J. O. M.; Gervasio, D. *J. Electrochem. Soc.* **1986**, *133*, 2262.
(9) (a) Baranov, A. I.; Shuvalov, L. A.; Shchagina, N. M. *JETP Lett.* **1988**, *36*, 459. (b) Munch, W.; Kreuer, K. D.; Traub, U.; Maier, J. *J. Mol. Struct.* **1996**, *381*, 1.
(10) (a) Haile, S. M.; Boysen, D. A.; Chisholm, C. R. I.; Merle, R. B. *Nature* **2001**, *410*, 910. (b) Boysen, D. A.; Uta, T.; Chisholm, C. R. I.; Haile, S. M. *Science* **2004**, *303*, 68.
(11) Jin, Y.; Fujiwara, K.; Hibino, T. *Electrochem. Solid-State Lett.* **2010**, *13*, B8.
(12) Hagiwara, R.; Nohira, T.; Matsumoto, K.; Tamba, Y. *Electrochem. Solid-State Lett.* **2005**, *8*, A231–A233.
(13) Lee, J. S.; Nohira, T.; Hagiwara, R. *J. Power Sources* **2007**, *171*, 535–539.
(14) Bureekaew, S.; Horike, S.; Higuchi, M.; Mizuno, M.; Kawamura, T.; Tanaka, D.; Yanai, N.; Kitagawa, S. *Nat. Mater.* **2009**, *8*, 831.

of water is much higher than that of the acid (Scheme 1a). Usually, there exist excess water molecules that form hydrogen bonding networks. Hence, proton conduction occurs via both the vehicle mechanism, where hydronium cations migrate by themselves, and the Grotthuss mechanism, where proton-exchange reactions take place between hydronium cations and water molecules via hydrogen bonding networks.[15] Kreuer et al. estimated the contribution of the Grotthuss mechanism to proton conduction in an acidic aqueous system.[15] In water-swollen polyelectrolyte membranes, excess water molecules are also necessary to form proton conduction channels.[16] In these aqueous systems, water molecules play the role of the proton carrier; however, at the same time, they lower the thermal stability of the system and restrict the operation temperatures of the fuel cells to less than 100 °C (typically <80 °C).

Ionic liquids (ILs) are ambient-temperature molten salts consisting entirely of ions. Because of their unique properties[17] such as low vapor pressure, high thermal stability, wide electrochemical windows, and high ionic conductivity, certain ILs are possible candidates for next-generation electrolytes of electrochemical devices, including lithium batteries,[18] electric double-layer capacitors,[19] actuators,[20] and dye-sensitized solar cells.[21] We reported for the first time that protic ILs, prepared through the neutralization reaction of a Brønsted acid and Brønsted base, can be employed as electrolytes for nonhumidified fuel cells.[22] In other words, protic ILs can exhibit fast proton transport and facile electrode reactions (hydrogen oxidation reactions (HORs) and oxygen reduction reactions (ORRs)) at the electrode interface under nonhumidified conditions. Since this report, the use of protic ILs as electrolytes in nonhumidified fuel cells has received attention from different groups.[23,24] If one compares acid−base reactions for an acidic aqueous system and protic IL system (Scheme 1b), a Brønsted base in the latter, typically amine, plays the role of water (the proton carrier) in the former. A difference is that there is no excess base in protic ILs. The thermal stability of protic ILs is dominated by the amount of neutral species (i.e., free acid and base), which is determined by the acid−base equilibrium constants. Angell and co-workers suggested that the difference between pK_a values of an acid and base is a good indicator of the equilibrium.[23] Ishiguro and co-workers investigated the acid−base equilibrium constant (K_s = [acid][base]) using the potentiometric titration technique.[25] They reported that K_s of a typical protic IL, ethylammonium nitrate, is $10^{-10.0}$. The thermal decomposition temperature (T_d) of protic ILs increases as the difference between pK_a values of an acid and base increases or as K_s values decrease. Dai and co-workers reported that protic ILs based on phosphazene or bicyclic guanidine superbases exhibit high thermal stability comparable to that of aprotic ILs.[26]

Since the first finding of the possibility of a protic IL-FC, we have investigated more than 80 different protic ILs and found that diethylmethylammonium trifluoromethanesulfonate ([dema][TfO]) possesses favorable bulk properties as well as facile interfacial electrochemical activity.[27] [dema][TfO] has a wide and stable liquid-temperature range (T_m = −6 °C and T_d = 360 °C) and high ionic conductivity (σ = 53 mS cm^{-1} at 150 °C and σ = 10 mS cm^{-1} even at room temperature) under anhydrous conditions. HORs and ORRs occur with small overpotentials in [dema][TfO], and consequently, the open-circuit voltage (OCV) of a H_2/O_2 IL-fuel cell at 150 °C without humidification is 1.03 V, which is close to the theoretical OCV (1.15 V). We also studied the fabrication of [dema][TfO] as membranes using sulfonated polyimides (SPIs) with the view to realizing practical fuel cells.[28] This paper deals with the characterization of protic ILs as anhydrous proton conductors and the development of a membrane-type fuel cell system operating under nonhumidified conditions at intermediate temperatures.

2. Experimental Section

Materials. 1,4,5,8-Naphthalene tetracarboxylic dianhydride (NTDA) (90%, Aldrich) was soaked in dimethylformamide (DMF) while stirring at 60 °C for 12 h. After filtration, NTDA was washed with acetone and dried in a vacuum. 2,2′-Benzidinesulfonic acid (BDSA) (70%, Tokyo Kasei) was washed with water and dissolved in water by adding triethylamine. Acidification with 1 M H_2SO_4(aq) afforded the precipitation of pure BDSA. Bis[4-(3-aminophenoxy)-phenyl]sulfone (3BAPPS) (95%, Wako Chem.) was recrystallized from ethanol. NTDA, BDSA, and 3BAPPS were dried in a vacuum oven at 80 °C prior to use. *m*-Cresol (98%, Wako Chem.) was dried over 4Å molecular sieves (Wako Chem.) prior to use. Triethylamine (TEA) (95%, Aldrich), *N*,*N*-diethylmethylamine (DEMA) (97%, Aldrich), *N*,*N*,*N*′,*N*′-tetramethylethylenediamine (TEMEDA) (98%, Tokyo Kasei), bis(trifluoromethanesulfon)amide ($HNTf_2$) (Morita Chem.), *N*,*N*-dimethylformamide (99.5%, Wako Chem.), and benzoic acid (99.5%, Junsei Chem.) were used as received. [dema][TfO] and [dema][NTf_2] were prepared by direct neutralization of the Brønsted acid and base according to a previously reported method[27] and dried in a vacuum oven at 80 °C for 24 h.

(15) (a) Dippel, T.; Kreuer, K. D. *Solid State Ionics* **1991**, *46*, 3. (b) Kreuer, K. D. *Solid State Ionics* **1997**, *94*, 55.
(16) (a) Roy, A.; Lee, H.-S.; McGrath, J. E. *Polymer* **2008**, *49*, 5037. (b) Bae, B.; Yoda, T.; Miyatake, K.; Uchida, H.; Watanabe, M. *Angew. Chem., Int. Ed.* **2010**, *49*, 317.
(17) (a) Welton, T. *Chem. Rev.* **1999**, *99*, 2071. (b) Wasserscheid, P.; Keim, W. *Angew. Chem., Int. Ed.* **2000**, *39*, 3772. (c) *Ionic Liquids in Synthesis*; Wasserscheid, P., Welton, T., Eds.; Wiley-VCH Verlag: Weinheim, 2003. (d) Plechkova, N. V.; Seddon, K. R. *Chem. Soc. Rev.* **2008**, *37*, 123.
(18) (a) Matsumoto, H.; Sakaebe, H.; Tatsumi, K.; Kikuta, M.; Ishiko, E.; Kono, M. *J. Power Sources* **2006**, *160*, 1308. (b) Seki, S.; Kobayashi, Y.; Miyashiro, H.; Ohno, Y.; Usami, A.; Mita, Y.; Watanabe, M.; Terada, N. *Chem. Commun.* **2006**, 544.
(19) (a) Nanjundiah, C.; McDevitt, S. F.; Koch, V. R. *J. Electrochem. Soc.* **1997**, *144*, 3392. (b) Barisci, J. N.; Wallace, G. G.; MacFarlane, D. R.; Baughman, R. H. *Electrochem. Commun.* **2004**, *6*, 22.
(20) (a) Lu, W.; Fadeev, A. G.; Qi, B.; Smela, E.; Mattes, B. R.; Ding, J.; Spinks, G. M.; Mazurkiewicz, J.; Zhou, D.; Wallace, G. G.; MacFarlane, D. R.; Forsyth, S. A.; Forsyth, M. *Science* **2002**, *297*, 983. (b) Fukushima, T.; Asaka, K.; Kosaka, A.; Aida, T. *Angew. Chem., Int. Ed.* **2005**, *44*, 2410.
(21) (a) O'Regan, B.; Grätzel, M. *Nature* **1991**, *353*, 737. (b) Papageorgiou, N.; Athanassov, Y.; Armand, M.; Bonhôte, P.; Patterson, H.; Azam, A.; Grätzel, M. *J. Electrochem. Soc.* **1996**, *143*, 3099. (c) Kawano, R.; Watanabe, M. *Chem. Commun.* **2003**, 330. (d) Kawano, R.; Matsui, H.; Matsuyama, C.; Sato, A.; Susan, M. A. B. H.; Tanabe, N.; Watanabe, M. *J. Photochem. Photobiol., A* **2004**, *164*, 87.
(22) (a) Noda, A.; Susan, M. A. B. H.; Kudo, K.; Mitsushima, S.; Hayamizu, K.; Watanabe, M. *J. Phys. Chem. B* **2003**, *107*, 4024. (b) Susan, M. A. B. H.; Noda, A.; Mitsushima, S.; Watanabe, M. *Chem. Commun.* **2003**, 938.
(23) (a) Yoshizawa, M.; Xu, W.; Angell, C. A. *J. Am. Chem. Soc.* **2003**, *125*, 15411. (b) Belieres, J.-P.; Gervasio, D.; Angell, A. C. *Chem. Commun.* **2006**, 4799. (c) Belieres, J.-P.; Angell, C. A. *J. Phys. Chem. B* **2007**, *111*, 4926.
(24) (a) Iojoiu, C.; Judeinstein, P.; Sanchez, J.-Y. *Electrochim. Acta* **2007**, *53*, 1395. (b) Judeinstein, P.; Iojoiu, C.; Sanchez, J.-Y.; Ancian, B. *J. Phys. Chem. B* **2008**, *112*, 3680. (c) Di Notto, V.; Negro, E.; Sanchez, J.-V.; Iojoiu, C. *J. Am. Chem. Soc.* **2010**, *132*, 2183.
(25) Kanzaki, R.; Uchida, K.; Hara, S.; Umebayashi, Y.; Ishiguro, S.-i.; Nomura, S. *Chem. Lett.* **2007**, *36*, 684.
(26) Luo, H.; Baker, G. A.; Lee, J. S.; Pagni, R. M.; Dai, S. *J. Phys. Chem. B* **2009**, *113*, 4181.
(27) Nakamoto, H.; Watanabe, M. *Chem. Commun.* **2007**, 2539.
(28) Lee, S.-Y.; Yasuda, T.; Watanabe, M. *J. Power Sources* **2010**, *195*, 5909.

Scheme 2. Synthetic Procedure for Sulfonated Polyimide in Diethylmethylammonium Form

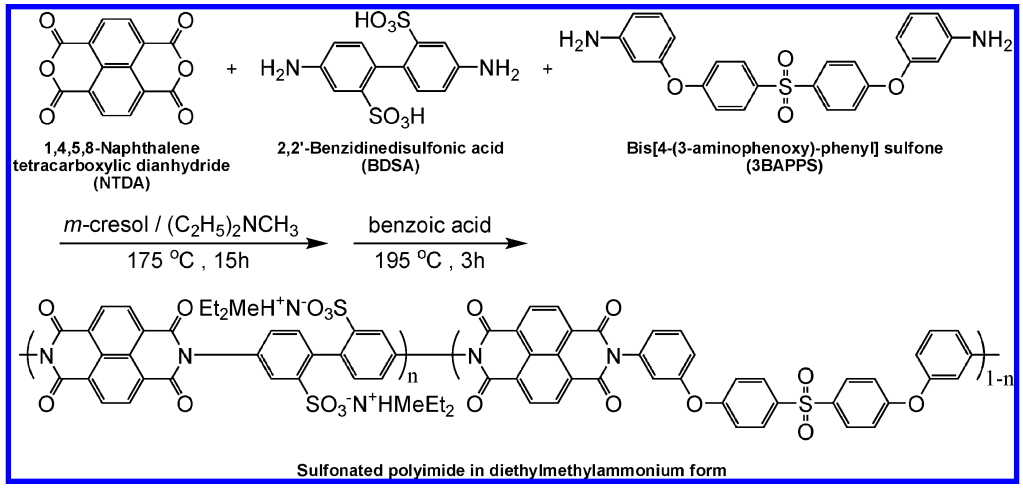

Synthesis of Sulfonated Polyimide (SPI). The synthetic route of SPI is shown in Scheme 2. SPIs with different ionic exchange capacities (IECs) were prepared by changing the molar ratios of diamine comonomers in the feed. Typically, BDSA (1.00 g, 2.9 mmol), 3BAPPS (1.26 g, 2.9 mmol), DEMA (0.73 g, 7.2 mmol), and 20 mL of *m*-cresol were added to a 100 mL three-necked flask equipped with a magnetic stirring bar. DEMA was added to the polymerization mixture to dissolve the BDSA in the solvent, and consequently, SPIs were obtained in diethylmethylammonium form. The mixture was stirred for several minutes under a nitrogen atmosphere at 100 °C until it completely dissolved. After NTDA (1.56 g, 5.8 mmol) was added to the flask, the mixture was heated to 175 °C and then stirred for 15 h. Benzoic acid (1.77 g, 14.5 mmol) was added, and the mixture was stirred at 195 °C for another 3 h to complete the imidization reaction. After the reaction, the mixture was cooled to 100 °C, and another 70 mL of *m*-cresol was then added to dilute the highly viscous solution. The solution was slowly poured into 500 mL of acetone. The resulting yellow fibrous precipitate was washed for 5 h with acetone to remove *m*-cresol completely and dried in a vacuum oven at 80 °C.

Fabrication of SPI/Protic IL Composite Membranes. The composite membranes were fabricated employing the solution casting method. Appropriate amounts of [dema][TfO], SPI powder, and *m*-cresol were added to a sample bottle equipped with a magnetic stirring bar. The mixture was stirred overnight at room temperature so that it dissolved completely, and the solution was then cast on a Petri dish. Evaporation of *m*-cresol at 60 °C gave a uniform composite membrane. The composite membranes were peeled from the Petri dish, dried in a vacuum oven at 80 °C for 24 h, and then stored in an argon atmosphere glovebox (VAC, [O_2] < 1 ppm, [H_2O] < 1 ppm).

Material Characterization. ^{1}H NMR spectra were recorded with a spectrometer (JEOL AL-400, 400 MHz). Measurements were performed using a double tube (SC-008, Shigemi Co. Ltd.; inner tube, 2.5 mm i.d., 3.29 mm o.d.; outer tube, 4.2 mm i.d., 4.965 mm o.d.; spacer, 3.3 mm i.d., 4.19 mm o.d.) with the sample in the inner tube and DMSO-d_6 containing TMS as the standard in the outer tube. Gel permeation chromatography was carried out using an HPLC system (Shimadzu) equipped with two columns (Shodex KD-803 and KD-804). 0.01 M LiBr in dimethylformamide was used as the eluent at a flow rate of 1 mL min^{-1}. The analyte solutions were filtered through a PTFE filter (pore size of 0.2 μm) before being injected into the columns. The molecular weights of the obtained polymers were calculated using a calibration curve based on polystyrene standards.

Self-Diffusion Coefficient. The self-diffusion coefficients of the ions in protic ILs were determined by pulsed-gradient spin−echo (PGSE)-NMR measurements, which were made using a JEOL GSH-200 spectrometer with a 4.7 T wide-bore superconducting magnet controlled by a TecMAG Galaxy system equipped with JEOL pulse field gradient probes and a current amplifier. The ^{19}F and ^{1}H spectra were measured with a ^{19}F/^{1}H probe. Each sample was placed in a 5 mm (o.d.) NMR microtube (BMS-005J, Shigemi Co. Ltd.) to a height of 5 mm. After a 90° pulse and longitudinal relaxation time (T_1) and transversal relaxation time (T_2) measurements, the self-diffusion coefficients were measured employing a simple Hahn spin−echo sequence (i.e., 90°−τ−180°−τ−acquisition), incorporating a gradient pulse in each τ period. The free-diffusion echo signal attenuation, E, can be expressed as the Stejskal equation

$$\ln E = \ln(S/S_{g=0}) = -\gamma^2 D g^2 \delta^2 (\Delta - \delta/3)$$

where S is the spin−echo signal intensity, δ is the duration of the field gradient with magnitude g, γ is the gyromagnetic ratio, D is the self-diffusion coefficient, and Δ is the interval between the leading edges of the gradient pulses and is fixed at 50 ms in this study. A recycle delay sufficient to allow full relaxation (i.e., >3T_1) was employed between each transition. The measurements of the cationic and anionic self-diffusion coefficients in each composition were made using ^{1}H (399.7 MHz) and ^{19}F (376.1 MHz) nuclei, respectively. The measurements were carried out with cooling from 130 to 30 °C, and the sample was thermally equilibrated at each temperature for 30 min before a measurement.

Electrochemical Polarization. Cyclic voltammetry (CV) was conducted at 150 °C for both ionic liquids, using a two-compartment glass cell under a dry N_2, H_2, or O_2 gas-bubbling atmosphere. The working electrode was a Pt wire, and the counter electrode was a Pt-black wire. The reference electrode was Pt-black immersed in a testing IL with hydrogen bubbling as a reversible hydrogen electrode (RHE), and was placed close to the working electrode through a Luggin capillary. The surface area of the working electrode was estimated from the hydrogen desorption peak of the cyclic voltammetry recorded for a 1 M H_2SO_4 aqueous solution at 25 °C. CV for [dema][TfO] was measured again in this study, and the reproducibility was confirmed, while that for [dema][NTf_2] was cited from ref 27.

Thermal Properties. Differential scanning calorimetry (DSC) was carried out on a Seiko Instruments DSC 220C under a nitrogen atmosphere. The samples were tightly sealed in aluminum pans in the dry glovebox. The samples were heated to 150 °C and then cooled to −150 °C and heated again to 150 °C at cooling and heating rates of 10 °C min^{-1}. The DSC was recorded during the reheating scans. Thermogravimetric analysis (TGA) of the composite membranes was performed using a Seiko Instruments TG-DTA 6200C under a nitrogen atmosphere. The samples were weighed and placed in aluminum pans and then heated from room temperature to 550 °C at a heating rate of 10 °C min^{-1}.

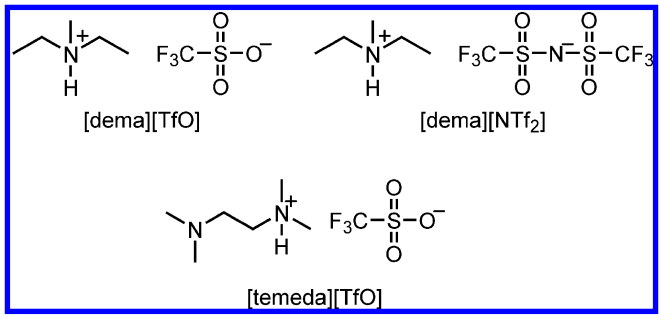

Figure 1. Chemical structures of [dema][TfO], [dema][NTf_2], and [temeda][TfO].

Mechanical Properties. A tensile strength−elongation test was carried out using a Micro 350 universal testing machine (Testometric, UK) equipped with a load cell of 500 kg f. The test specimens were carefully cut to have dimensions of 4 mm × 60 mm, and the thickness of each specimen was measured. The specimens were set between the 40-mm-separated clips of the testing machine and were measured with a constant crosshead speed of 2 mm min^{-1}. Stress−strain curves were recorded by a computer.

Gas Permeability. Hydrogen and oxygen permeability through the composite membranes was measured by using the equal-pressure method and a GTR-Tech 10XFKS gas permeation tester equipped with a Yanaco G2700T gas chromatograph. The composite membranes were cut to a diameter of 30 mm and set in a cell with a gas inlet and outlet on either side of the membrane. The test was carried out using dry hydrogen and oxygen at 30, 50, and 80 °C.

Ionic Conductivities. Ionic conductivities of protic ILs and the composite membranes were determined employing the complex impedance method in the temperature range from 40 to 160 °C. A protic IL was placed in a dip-type glass cell with two Pt rods fixed at a constant electrode distance in the glovebox. The cell constant was determined using a 0.1 M KCl standard aqueous solution and found to be 3.0 cm^{-1} at 30 °C. The composite membranes were cut into strips 6−7 mm wide and 10 mm long and set on two platinum-wire-electrode cells; the electrodes were separated by a distance of 4 mm and arranged in parallel on the cells. The cells were placed in an oven and thermally equilibrated at each temperature for 1.5 h before the measurements. The measurements were carried out with a potentiostat (Autolab, PGSTAT30) in the frequency range of 1 Hz to 10 MHz under anhydrous conditions.

Fabrication of Membrane Electrode Assembly (MEA) and Single-Cell Test. A single-cell test of the composite membrane was performed using a gas diffusion electrode (E-TEK GDE, LT-140EW; 30% Pt on Vulcan XC-72, 0.5 mg cm^{-2}, ionomer free). An MEA was simply fabricated by sandwiching a composite membrane between the two gas diffusion electrodes. The MEA was tested in a single cell with a serpentine-shaped gas flow field and an active area of 4 cm^2 at ambient pressure. The H_2/O_2 fuel cell polarization curves were determined at 30, 120, and 140 °C using an Eiwa Corp. FC test station. Anhydrous H_2 (99.99%) and O_2 (99.6%) gases were supplied to the test station without humidification.

3. Results and Discussion

3.1. Characterization of Protic ILs as Proton Conductors. Bulk Properties. For a better understanding of protic ILs as FC electrolytes, we focused on [dema][TfO] and diethylmethylammonium bis(trifluoromethanesulfon)amide ([dema][NTf_2]) (Figure 1) because they consist of a common cation with different anions, the conjugate acids of which are known as superstrong acids but categorized as oxoacid and imide acid, respectively. Both the protic ILs exhibit rather high ionic conductivity, reaching ca. 50 mS cm^{-1} at 150 °C and retaining ca. 10 mS cm^{-1} even at room temperature (see Supporting Information, Figure S1). No apparent difference in the ionic conductivity was observed except for an abrupt decrease in the conductivity for [dema][NTf_2] at ∼20 °C owing to its value of T_m (24 °C). The proton conduction mechanism and the transference number are significant factors in characterizing the electrolytes. We measured self-diffusion coefficients of N−H and C−H protons of the cation (protons) and C−F fluorine of the anion by using PGSE-NMR because the N−H proton is an exchangeable proton, and proton transport via both the vehicle mechanism and Grotthuss mechanism can contribute to the diffusion, whereas the C−H proton and C−F fluorine are not exchangeable; thus, only the vehicle mechanism can contribute to the diffusion.[22] Therefore, the difference in the diffusion coefficients of the N−H proton and C−H proton reflects proton transport via the Grotthuss mechanism.[22] Parts a and b of Figure 2 show the temperature dependence of the self-diffusion coefficients of the protic ionic liquids. The diffusion coefficients of the N−H proton and C−H proton in [dema][TfO] and [dema][NTf_2] are almost the same, suggesting that proton conduction basically occurs via the vehicle mechanism. It is also seen that the cationic diffusivity is greater than the anionic diffusivity for both ionic liquids. Figure 2c shows the temperature dependence of the transference number (t_+) of the cation (proton), which is calculated by dividing the diffusion coefficient of the N−H proton by the sum of cationic and anionic diffusivity (i.e., the sum of the diffusion coefficients of the C−H proton and C−F fluorine). At room temperature, transference numbers of the cation (proton) are 0.56 for [dema][TfO] and 0.62 for [dema][NTf_2]. With increasing temperature, the transference numbers of the cations in both protic ionic liquids tend to decrease, indicating that the activation energy for the diffusion of the anion is higher than that for the diffusion of the cation.[29] As well as ion transport properties, thermal stability is a significant property. As we previously reported, T_d is 360 °C for [dema][TfO] and 375 °C for [dema][NTf_2], while T_m is −6 and 24 °C, respectively.[27] These results indicate that [dema][TfO] and [dema][NTf_2] have similar bulk properties.

Interfacial Electrochemical Properties. In contrast to the case of the bulk properties, the electrochemical properties are completely different for [dema][TfO] and [dema][NTf_2]. Figure 3 shows the cyclic voltammograms at the first and second cycles under different conditions at 150 °C. When hydrogen gas is bubbled into [dema][TfO] around the working electrode, the oxidative current corresponding to the HOR stands up at ca. 0.4 V in the first cycle, and from the second cycle, the oxidative current sharply stands up at 0 V (vs RHE). In protic ILs, the acceptor of the proton generated by the HOR is either the anion or amine. In the first cycle of the potential scan, protons generated by the HOR are accepted by [TfO] anions because there is almost no free amine because of the large equilibrium constant of the proton transfer reaction. Because the anion is a much weaker base than the amine, the overpotential of the HOR is large. During the first potential cycle, amine is generated at the counter electrode and plays the role of a proton acceptor from the second potential cycle, and thus, the overpotential becomes low. Friesen and co-workers observed the same behavior and suggested that the differences in the onset potentials of the HOR between the first cycle and the latter cycles can be converted to acid−base equilibrium constants.[30] When oxygen is bubbled in [dema][TfO], a reductive current corresponding to the ORR can be clearly observed at ca. 1.0 V

(29) (a) Tokuda, H.; Hayamizu, K.; Ishii, K.; Susan, M. A. B. H.; Watanabe, M. *J. Phys. Chem. B* **2004**, *108*, 16593. (b) Noda, A.; Hayamizu, K.; Watanabe, M. *J. Phys. Chem. B* **2001**, *105*, 4603.

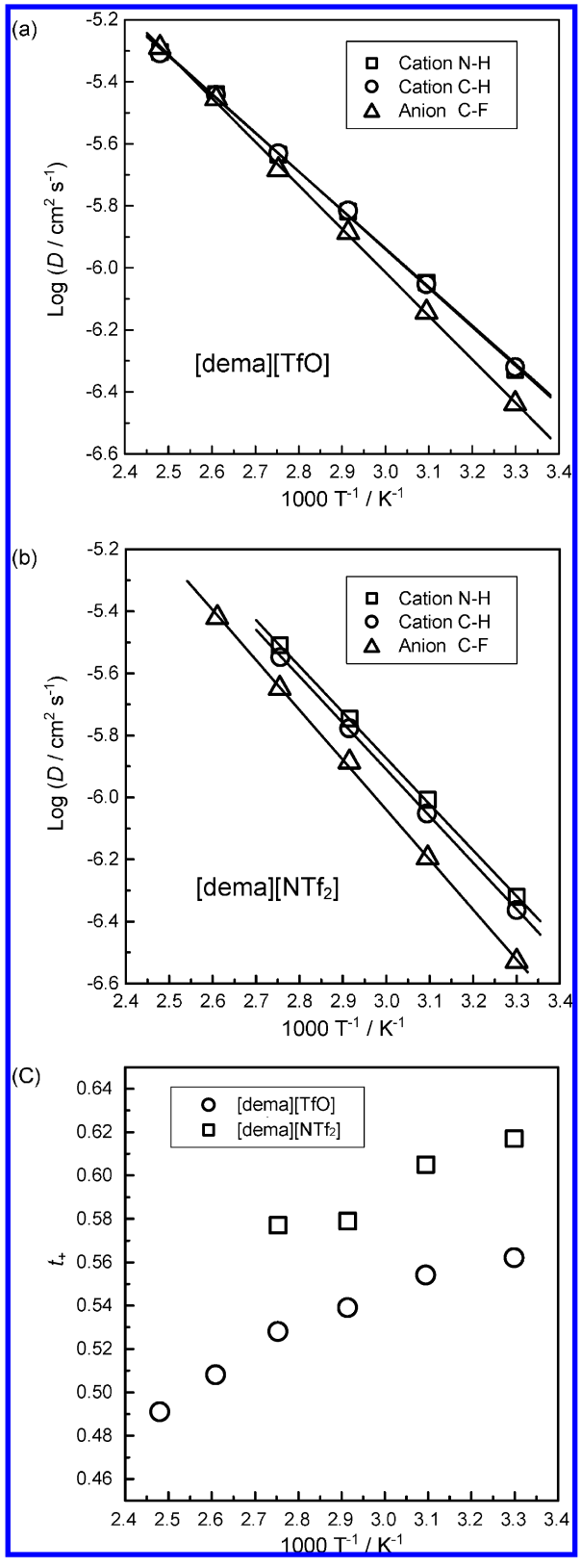

Figure 2. Diffusion coefficients, D, of cation C−H and N−H protons and anion ^{17}F for [dema][TfO], (a), and for [dema][NTf_2], (b); and proton transference number, t_+, in these PILs, (c).

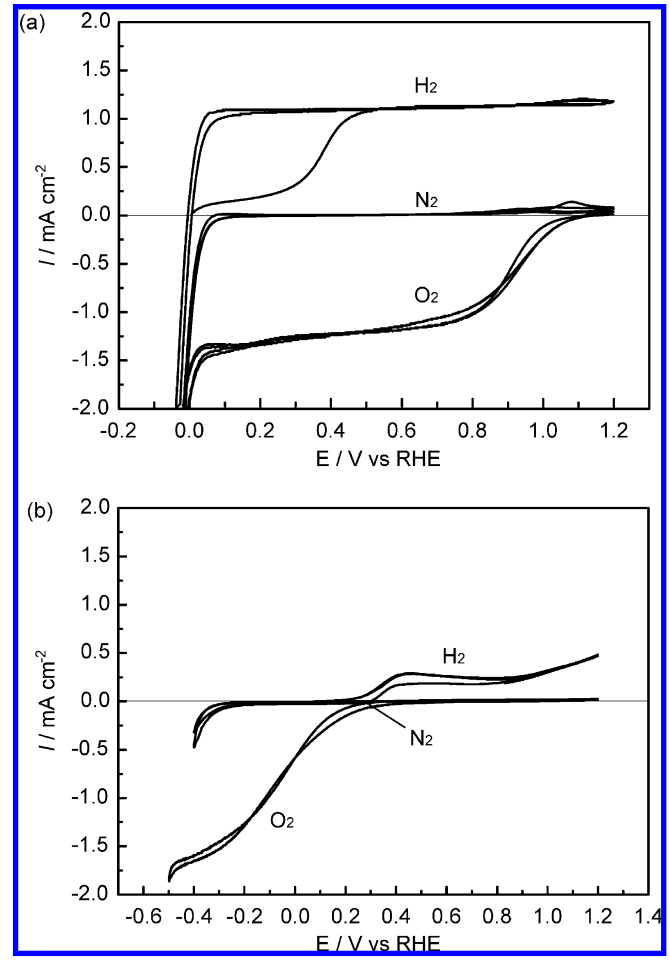

Figure 3. Cyclic voltammograms of (a) [dema][TfO] and (b) [dema][NTf_2] using a Pt wire working electrode under H_2, O_2, or N_2 gas bubbling conditions. Scan rate is 10 mV s^{-1}, and gas feed is 2 mL min^{-1}. The voltammogram for [dema][NTf_2] is cited from ref 27.

vs RHE. The OCV of a H_2/O_2 liquid fuel cell using [dema][TfO] is higher than 1 V at 150 °C, as we previously reported.[27] In contrast to [dema][TfO], [dema][NTf_2] has quite poor activity for both the HOR and ORR. The onset potential of the HOR does not change even after the second cycle. In addition, the onset potential of the ORR is much more negative than that for [dema][TfO]. The OCV for [dema][NTf_2] is determined as ca. 0.7 V. These observations suggest that the protic ILs have similar bulk properties but exhibit quite different electrochemical activities.

Proton Transport under Fuel Cell Operation. t_+ is an important parameter in determining the performance of the electrolyte of a fuel cell. In the case of hydrated sulfonated polymer electrolyte membranes such as Nafion, t_+ is 1.0 because the counteranions, sulfonate groups, are affixed to the polymer backbone. For PPA/PBI, proton conduction occurs almost completely via the Grotthuss mechanism and t_+ is confirmed to be 0.98.[31] On the other hand, t_+ of the present protic ILs is 0.5−0.6, as shown in Figure 2c. This is unfavorable for an electrolyte of a fuel cell because a low t_+ results in not only low proton conductivity but also polarization of the fuel cells. However, the proton conduction mechanism in the protic ILs under fuel cell operation can differ from that in the bulk because

(30) Bautista-Martinez, J. A.; Tang, L.; Belieres, J.-P.; Zeller, R.; Angell, C. A.; Friesen, C. *J. Phys. Chem. C* **2009**, *113*, 12586.
(31) (a) Li, Q.; Jensen, J. O.; Savinell, R. F.; Bjerrum, N. J. *Prog. Polym. Sci.* **2009**, *34*, 449. (b) Jayakody, J. R. P.; Chung, S. H.; Durantino, L.; Zhang, H.; Xiao, L.; Benicewicz, B. C.; Greenbaum, S. G. *J. Electrochem. Soc.* **2007**, *154*, B242.

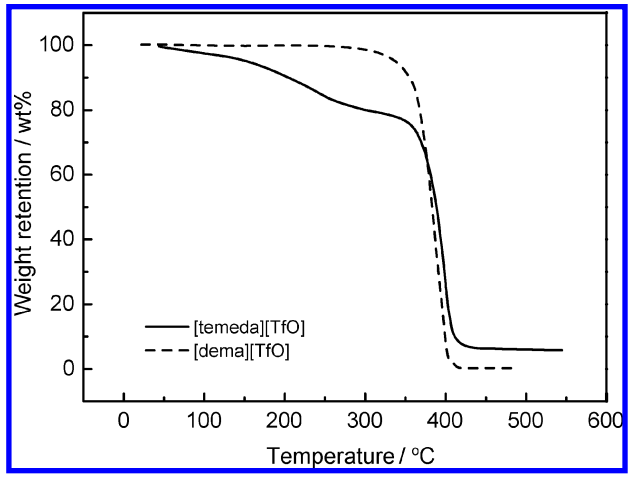

Figure 4. Thermogravimetric curves of [temeda][TfO] and [dema][TfO].

Scheme 3. Intra- and Intermolecular Proton Exchange Reactions of [temeda][TfO]

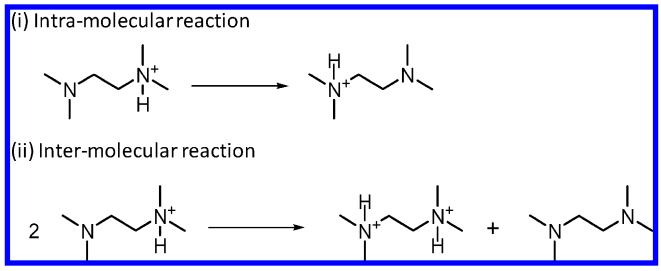

the free amine, diethylmethylamine, is continuously generated at the cathode by the ORR between [dema] and oxygen to generate water. The free amine can accept a proton and thus a proton-exchange reaction between the free amine and [dema] is possible.

To confirm such a possibility, we prepared a model compound, dimethylaminoethyldimethylammonium trifluoromethane sulfonate ([temeda][TfO]) by the neutralization reaction of *N*,*N*,*N*′,*N*′-tetramethylethylenediamine and trifluoromethanesulfonic acid at a ratio of 1:1 (Figure 1). [temeda][TfO] has both ammonium and amine groups in the same cationic structure, and thus, it appears to simulate the circumstance of the protic ILs where the cathodic reaction occurs. Figure 4 shows thermogravimetric curves of [temeda][TfO] and [dema][TfO]. While the weight loss of [dema][TfO] starts at ∼350 °C, that of [temeda][TfO] starts around 100 °C and a second weight loss is observed at ∼350 °C. Such low T_d, corresponding to the first weight loss, cannot be explained by [temeda][TfO] forming from the combination of an amine and a superstrong acid, where ΔpK_a is similar to that of [dema][TfO]. The first weight loss corresponds to the amount of *N*,*N*,*N*′,*N*′-tetramethylethylenediamine, which is generated by the formation of the diammonium cation due to the intermolecular proton transfer reaction (Scheme 3, bottom). The generated diamine easily evaporates because of its rather low boiling point (T_b = 122 °C). Figure 5 shows the ^{1}H NMR spectrum of [temeda][TfO] with the assignment. It is revealed that protons of methyl groups, which are attached to the amine (a) and ammonium nitrogen atoms (a′), cannot be distinguished, indicating that a fast proton-exchange reaction occurs between the ammonium and amine groups (Scheme 3, top). The inset of Figure 5 shows a change in the ratio of 1/12 (corresponding to a single proton) of the number of integrated methyl protons (a + a′) to the number of integrated ammonium protons (c) when [temeda][TfO] is evacuated at 120 °C. A ratio of unity (1.00) means that the cation has one ammonium proton. The ratio gradually increases and reaches 1.4 after 180 h, indicating that the amount of diammonium cation gradually increases during the experiment (Scheme 3, bottom). These results indicate that a proton-exchange reaction between the ammonium cation and free amine is possible if they coexist.

Our liquid fuel cells and membrane-type fuel cells using [dema][TfO] can be operated for a long time without decomposition of the protic IL (*vide infra*). During the fuel cell operation, the free amine is continuously generated. If there is no proton-exchange reaction, the free amine diffuses back to the anode and accepts the protons generated in the HOR. Judging from the diffusivity of the cation (Figure 2), it takes roughly 10^4 s for amine to diffuse over 1 mm distance. Because the free amine is thermally quite unstable (T_b = 64 °C), it easily evaporates, resulting in the decomposition of the electrolyte. Therefore, it is quite plausible that the proton-exchange mechanism is responsible for the proton transport under fuel cell operation.

3.2. Membrane Fabrication and Fuel Cell Operation. Synthesis and Fabrication of Composite Membrane. We have proposed that certain combinations of ionic liquids and polymers are highly compatible and the network polymers can retain the ionic liquids to produce ion gels.[32] In the case of the polymer electrolyte membrane in a fuel cell, however, a number of properties of the membrane are required, including high proton conductivity, high thermal and chemical stability, reliable mechanical properties, and low gas (H_2, O_2) permeability. In this study, we focused on SPI[33] as a matrix polymer owing to its high thermal stability, film formability, high mechanical strength, and low gas permeability. In a previous paper,[28] it was reported that five-membered SPIs in diethylmethylammonium form have good compatibility with [dema][TfO] and gave transparent, ductile, and mechanically stable composite membranes. Furthermore, fuel cell operation under nonhumidified conditions was demonstrated using the composite membrane. However, fuel cell operation above 100 °C could not be achieved because degradation of the composite membranes via hydrolysis occurs at high temperature. In this report, six-membered SPIs that are more stable against hydrolysis[34] were employed as matrix polymer. SPIs with different IECs, 1.41 meq g^{-1} and 2.15 meq g^{-1}, were successfully synthesized in diethylmethylammonium form (Scheme 2). Fundamental characteristics of the six-membered SPIs are listed in Table 1. To confirm hydrolytic stability, membranes of the six- and five-membered SPIs in diethylmethylammonium form were immersed in hot water (90 °C). It was confirmed that the six-membered SPIs exhibited no weight loss even with immersion for 10 days, whereas the five-membered SPIs completely dissolved within a day. This result obviously indicates higher

(32) (a) Susan, M. A. B. H.; Kaneko, T.; Noda, A.; Watanabe, M. *J. Am. Chem. Soc.* **2005**, *127*, 4976. (b) Noda, A.; Watanabe, M. *Electrochim. Acta* **2000**, *45*, 1265.
(33) (a) Yin, Y.; Suto, Y.; Sakabe, T.; Chen, S.; Hayashi, S.; Mishima, T.; Yamada, O.; Tanaka, K.; Kita, H.; Okamoto, K. *Macromolecules* **2006**, *39*, 1189. (b) Asano, N.; Aoki, M.; Suzuki, S.; Miyatake, K.; Uchida, H.; Watanabe, M. *J. Am. Chem. Soc.* **2006**, *128*, 1762. (c) Peckham, T. J.; Schmeisser, J.; Rodgers, M.; Holdcroft, S. *J. Mater. Chem.* **2007**, *17*, 3255. (d) Essafi, W.; Gebel, G.; Mercier, R. *Macromolecules* **2003**, *37*, 1431.
(34) (a) Genies, C.; Mercier, R.; Sillion, B.; Cornet, N.; Gebel, G.; Pineri, M. *Polymer* **2001**, *42*, 359. (b) Genies, C.; Mercier, R.; Sillion, B.; Petiaud, R.; Cornet, N.; Gebel, G.; Pineri, M. *Polymer* **2001**, *42*, 5097.

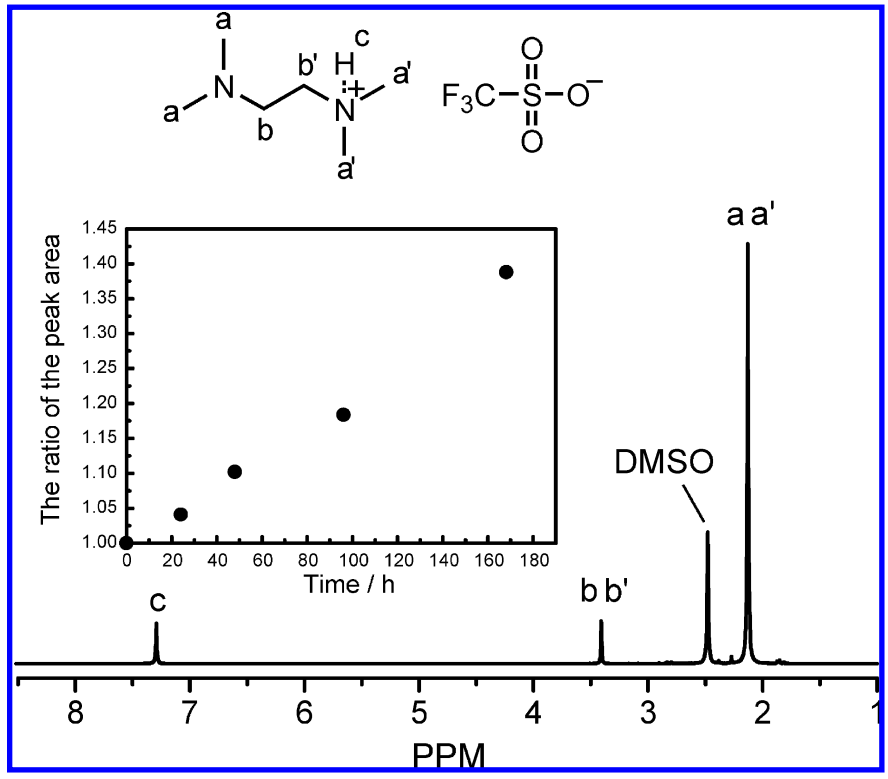

Figure 5. [1]H NMR spectrum of [temeda][TfO]. The inset shows a change in the ratio of 1/12 (corresponding to the single proton) of the integrated methyl protons (a + a′) to the integrated ammonium proton (c) when [temeda][TfO] is evacuated at 120 °C.

Table 1. Molecular Characterization of SPIs

	mole fraction in feed							
polymer	NTDA	BDSA	3BAPPS	IEC[a] (meq g^{-1})	IEC[b] (meq g^{-1})	M_n[c] ($\times 10^5$)	M_w[d] ($\times 10^5$)	M_w/M_n[e]
SPI-1.41	0.5	0.25	0.25	1.41	1.41	2.42	5.38	2.22
SPI-2.15	0.5	0.40	0.10	2.18	2.15	3.79	9.42	2.48

[a] Ion exchange capacity calculated from feed monomer ratio. [b] Ion exchange capacity estimated from [1]H NMR spectra. [c] Number average molecular weight. [d] Weight average molecular weight. [e] Polydispersity index.

hydrolytic stability of the six-membered SPIs. Transparent, yellowish, and flexible composite membranes (Supporting Information, Figure S2) were fabricated by employing a solution casting method using *m*-cresol as the casting solvent. Scanning electron microscopy (data not shown) revealed that these composite membranes were not porous but pinhole-free and dense. The membranes are abbreviated as SPI-*X*(*Y*), where *X* and *Y* are the IEC value (meq g^{-1}) of the SPI matrix and the content of [dema][TfO] (wt %), respectively.

Thermal Properties. In the DSC analysis, the composite membranes including 33 wt % [dema][TfO] had no peak corresponding to the T_m for [dema][TfO], while pure [dema][TfO] had an endothermic peak corresponding to the T_m (Supporting Information, Figure S3). This indicates that the matrix polymer and [dema][TfO] are compatible at the [dema][TfO] content. However, the composite membrane based on the SPI with an IEC of 1.41 meq g^{-1} had a peak corresponding to T_m of [dema][TfO] at contents of [dema][TfO] higher than 67 wt %, while the composite membranes based on SPI with an IEC of 2.15 meq g^{-1} had no peak up to 75 wt %. The sulfonic acid groups in diethylmethylammonium form significantly affect the compatibility, and [dema][TfO] can be preferentially incorporated in the domain consisting of the ionic part of the polymers. In the TGA analysis (Supporting Information, Figure S4), the weight loss started at ~300 °C for all the composite membranes, which confirms sufficient thermal stability for fuel cell applications.

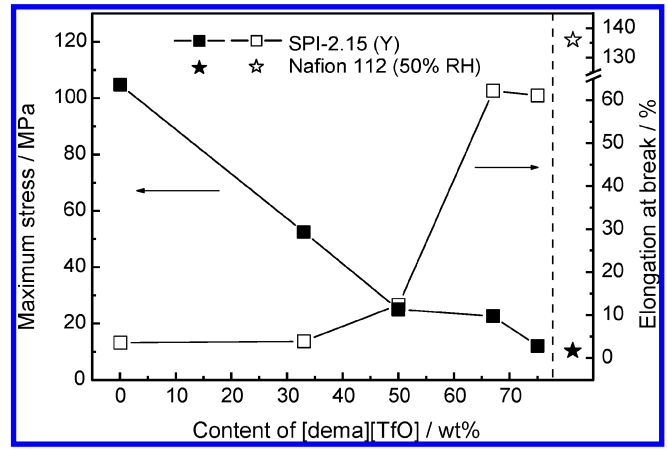

Figure 6. Tensile strength and elongation at break of SPI-2.15 composite membranes as a function of [dema][TfO] content at room temperature. The data for Nafion 112 at room temperature are cited from ref 32.

Mechanical Properties. Figure 6 shows the tensile strength and elongation at break as functions of [dema][TfO] content in the SPI-2.15 composite membranes at room temperature. The matrix polymer has an elongation at break of 3.6% and tensile strength of 105 MPa. The composite membranes become ductile

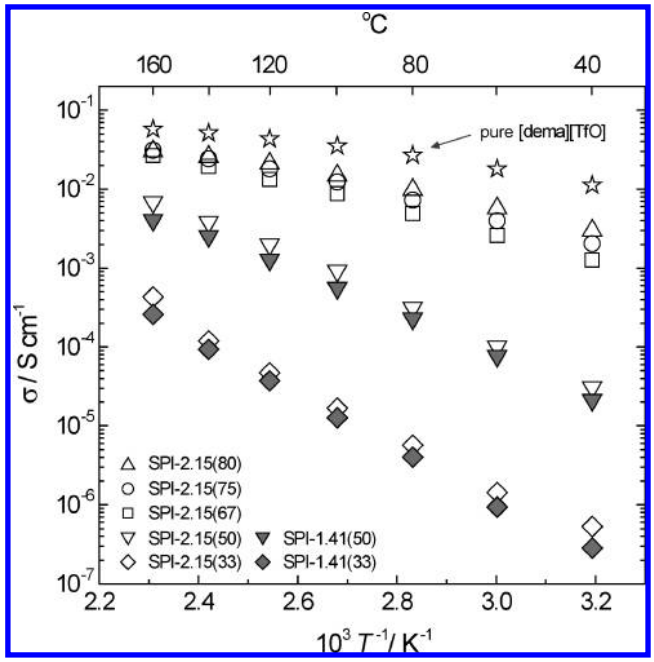

Figure 7. Arrhenius plots of ionic conductivity for pure [dema][TfO] and SPI/[dema][TfO] composite membranes with different [dema][TfO] contents.

as the content of [dema][TfO] increases and the elongation at break increases rapidly when the [dema][TfO] content is higher than 67 wt %. Comparing with the mechanical properties of hydrated Nafion,[35] the composite membrane including 75 wt % [dema][TfO] exhibited similar maximum stress with slightly lower elongation at break. An abrupt change in the elongation at break with increasing [dema][TfO] content (Figure 6) is consistent with the change in the ionic conductivity (*vide infra*) and thus may be related to the connectivity of the ion conduction channel.

Ionic Conductivity under Nonhumidified Conditions. The ionic conductivity of [dema][TfO] and the composite membranes was investigated in the temperature range from 40 to 160 °C under anhydrous conditions. Figure 7 shows Arrhenius plots of the ionic conductivities of the composite membranes based on SPI-1.41 and SPI-2.15, together with the data of pure [dema]-[TfO]. The composite membranes, including 33 wt % and 50 wt % [dema][TfO], exhibit low ionic conductivities ($<10^{-4}$ S cm^{-1} at 40 °C) with large temperature dependencies, while those with [dema][TfO] contents higher than 67 wt % exhibit fairly good ionic conductivity ($>10^{-3}$ S cm^{-1} at 40 °C) with low temperature dependencies. We assume that this is related to the connectivity of the ion-conducting channel in the membranes, and continuous connection is achieved in the membranes with [dema][TfO] contents higher than 67 wt %. Furthermore, the composite membranes based on SPI with an IEC of 2.15 meq g^{-1} exhibit higher ionic conductivity than those based on SPI with an IEC of 1.41 meq g^{-1}. This is due to the contribution of the diethylmethylammonium countercation to the ionic conductivity via the cation exchange reaction rather than the difference in the connectivity of the ion conduction channel because the temperature dependencies of the ionic conductivity of the composite membranes are almost the same.

Gas Permeability. Figure 8 shows the temperature dependence of dry hydrogen and oxygen permeability coefficients of the

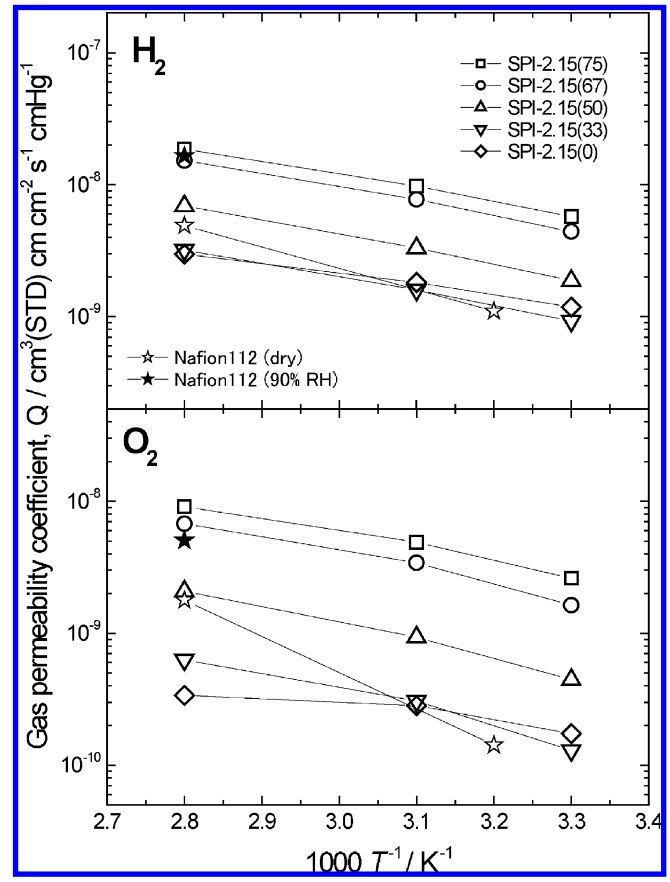

Figure 8. Arrhenius plots of dry hydrogen and oxygen permeability coefficients for SPI-2.15 composite membranes and Nafion 112 membranes cited from ref 31.

SPI-2.15 composite membranes containing different amounts of [dema][TfO]. The data for Nafion 112 under dry and humidified conditions are cited from the literature.[31] The gas permeability coefficients increase with increasing temperature for both composite membranes and Nafion membranes. The [dema][TfO] content significantly affects the gas permeability and a large increase is observed for the composite membranes when the [dema][TfO] content changes from 33 to 67 wt %. This behavior is again similar to that of the ionic conductivity and the mechanical properties. The gas permeability of the composite membranes including amounts of [dema][TfO] greater than 67 wt % is similar to that of the Nafion membranes under humidified conditions. It is concluded that the gas permeability of the composite membranes cannot be a serious disadvantage when they are used as electrolyte membranes (gas separation membranes) in fuel cells.

Single-Cell Test of Composite Membranes without Humidification. The H_2/O_2 fuel cell prepared using SPI-2.15(75) composite membranes with thicknesses of 55 μm was operated at 30 °C, 120 °C, and 140 °C without humidification. Note that ionomer-free gas diffusion electrodes, which are usually used for PAFCs, were employed in this system because Nafion ionomer does not work at high temperatures under nonhumidified conditions. Figure 9 shows the fuel cell polarization curves at different temperatures. At 30 °C, a current density higher than 630 mA cm^{-2} was achieved with a maximum power density of 187 mW cm^{-2} and an OCV of 0.83 V. At 120 °C, a current density higher than 250 mA cm^{-2} was observed with a maximum power density of 63 mW cm^{-2} and an OCV of 0.75 V. At 140 °C, the respective values were 90 mA cm^{-2}, 19 mW

(35) Lu, D.; Lu, W.; Li, C.; Liu, J.; Xu, J. *Solid State Ionics* **2006**, *177*, 1111.

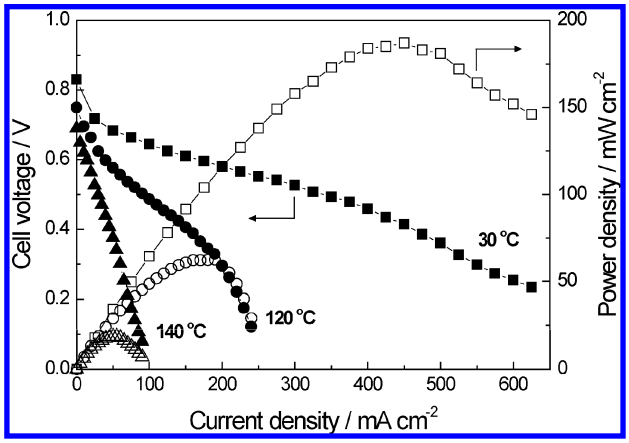

Figure 9. Polarization curves of a H_2/O_2 fuel cell using SPI-2.15(75) composite membrane without humidification: (■,□) operated at 30 °C, (●,○) operated at 120 °C, (▲,Δ) operated at 140 °C. Flow rate of reaction gases, H_2 and O_2, are 12 mL min^{-1} for 120 and 140 °C, while 120 mL min^{-1} and 60 mL min^{-1}, respectively, for 30 °C.

cm^{-2}, and 0.69 V. We consider that the reason why the fuel cell performance decreases with increasing temperature is not intrinsic because the limiting currents and the HOR and ORR potentials appearing in CVs of for [dema][TfO], as shown in Figure 3a, simply increase and do not greatly change, respectively, as the temperature increases to 150 °C (data not shown). In the membrane fuel cells, we suspect that a small amount of leaked protic ionic liquid plays the role of a proton conductor in the catalyzed gas-diffusion electrodes as phosphoric acid does in PAFCs. The mixture of [dema][TfO] and water generated during the fuel cell operation may form proton-conducting channels at the three-phase interface in the catalyst layer. However, the water easily evaporates at high temperature, and thus, utilization of the Pt catalyst decreases with increasing temperature, resulting in deterioration of the fuel cell performance at high temperature. Furthermore, the adhesion between the membrane and the catalyzed gas-diffusion electrodes is not sufficient at present. We believe that these problems can be solved by optimizing the electrode structure and/or employing a hydrophobic protic ionic liquid (e.g., ethylmethylpropylammonium nonafluoromethanesulfonate ([empa][NfO])).[36] Finally, the durability of the fuel cell was checked by keeping it in the OCV state with the continuous feeding of H_2 and O_2 gases at 120 °C without humidification using an SPI-2.15(50) membrane. Figure 10 shows the change in the OCV as a function of time. No decrease in the OCV is observed over 230 h. Although the results are only preliminary, the membrane-type IL fuel cell is believed to be promising and further work has commenced.

(36) Yasuda, T.; Ogawa, A.; Kanno, M.; Mori, K.; Sakakibara, K.; Watanabe, M. *Chem. Lett.* **2009**, *38*, 692.

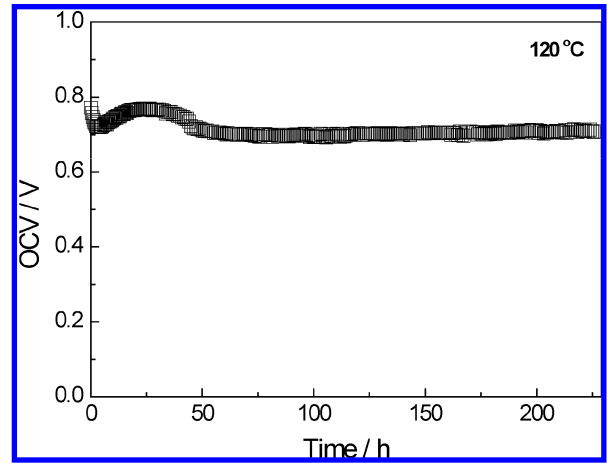

Figure 10. Change in OCV as a function of time for a fuel cell using SPI-2.15(50) composite membrane without humidification at 120 °C. Flow rate of both reaction gases (H_2 and O_2) are 12 mL min^{-1}.

4. Conclusions

In this paper, the characteristics of a protic ionic liquid as an anhydrous proton conductor and fabrication of a nonhumidified intermediate temperature fuel cell using the protic ionic liquid are described. [dema][TfO] possessed thermal property, ionic conductivity, and transport property similar to those of [dema][NTf_2]. However, it exhibited quite different behavior in terms of fuel cell electrode reactions (HORs and ORRs), and [dema][TfO] was more favorable as an electrolyte for a fuel cell than [dema][NTf_2]. It was revealed that fast proton-exchange reactions can occur when amine species are generated by the ORR, indicating that the polarization of a fuel cell system derived from a low proton transference number for [dema][TfO] can be avoided. By using six-membered SPIs, composite membranes including a large amount of [dema][TfO] were successfully fabricated. The composite membranes had favorable thermal properties, ionic conductivity, gas permeability, and mechanical properties. We succeeded in operating a nonhumidified fuel cell that employs a composite membrane at 30, 120, and 140 °C.

Acknowledgment. This work was financially supported by NEDO of Japan and Grant-in-Aid for Scientific Research in the Priority Area "Science of Ionic Liquid" from the MEXT of Japan. We thank Prof. Chang-kwon Moon for tensile testing and Dr. Kikuko Hayamizu for the assistance for measuring diffusion coefficients by PGSE-NMR. We also thank Kanagawa Industrial Technology Center for gas permeability test.

Supporting Information Available: Figures S1−S4. This material is available free of charge via the Internet at http://pubs.acs.org.

JA102367X